

УДК 581.1

EFFECTS OF UV-B, WATER DEFICIT AND THEIR COMBINATION ON *Bryum argenteum* PLANTS¹

© 2016 R. Hui*, R. Zhao**, L. Liu*, R. Zhu*, G. Li*, Y. Wei***

*Shapotou Desert Research and Experiment Station, Cold and Arid Region Environmental and Engineering Research Institute, Chinese Academy of Sciences, Lanzhou, Gansu, China

**School of Life Science, Lanzhou University, Lanzhou, China

***The University of Melbourne, Parkville, Australia

Received December 12, 2014

The changes in climate can result in several environmental stress factors. Among these, ultraviolet-B (UV-B) and water-deficit have serious detrimental effects on plants at the physiological, morphological, and biochemical levels. Biological soil crusts (BSCs), formed by an association between soil particles and photosynthetic algae, cyanobacteria, lichens, and mosses in varying proportions, are a key functional feature of arid and semi-arid areas. In this study, *Bryum argenteum*, isolated from BSCs found in the Tengger Desert, China, was subjected to UV-B and water-deficit, singly and in combination, in a greenhouse for 10 days. The treatments consisted of four UV-B levels (2.75, 3.08, 3.25, and 3.41 W/m²) and two water application levels (well-watered and water-deficit). UV-B treatment and water-deficit singly caused a significant decrease in chlorophyll (Chl) fluorescence parameters, carotenoid (Car), total flavonoid contents, and a significant increase in malondialdehyde (MDA) content. The combined application of UV-B and water-deficit produced significantly higher Chl fluorescence parameters, Chl, Car and total flavonoid contents, but reduced MDA content. These results suggest that water-deficit alleviates the negative effects on *B. argenteum* caused by enhanced UV-B radiation. Our results provide novel insights into understanding the relationships between BSCs and environmental factors, and supply a theoretical foundation for BSC assessment and protection in arid and semi-arid regions.

Keywords: *Bryum argenteum* – biological soil crusts (BSCs) – combined stress – chlorophyll fluorescence – photosynthetic pigments – ultraviolet-B (UV-B) – water-deficit

DOI: 10.7868/S0015330316020081

INTRODUCTION

The emission of ozone-depleting substances, through human activities, has resulted in increased levels of solar ultraviolet-B (UV-B, 280–320 nm) at the earth's surface, and has affected the global climate [1]. Previous studies have shown that increased UV-B levels have deleterious effects on economically important crop plants at the physiological, morphological, and biochemical levels [2]. Water-deficit caused by drought is also one of the main constraints to plant growth and survival, and induces photosynthetic physiological process modifications in plants.

Under natural conditions, plants usually exposed to a number environmental factors simultaneously, including inappropriate levels of CO₂, salinity, temperature, water, and heavy metals [3]. Therefore, further research on the relationship between UV-B and other environmental factors will lead to a more comprehensive understanding of plant responses to abiotic stress factors. The interaction between UV-B and other environmental factors may cause various responses in plants which can be additive, synergistic, or antagonistic [4].

Desiccation, temperature extremes, high pH, intense UV-B radiation, and high salinity environments in arid and semi-arid areas, restricts the growth of many types of vascular plants, but biological soil crusts (BSCs) develops and are widely spread across the soil surface. In many areas, they may constitute up to 70% of the living cover [5]. BSCs are a key functional component of arid and semi-arid areas, and are mainly composed of photosynthetic algae, cyanobacteria, lichens, and mosses [6]. They greatly improve soil formation, stability and fertility by preventing wind and/or water erosion. They supply nutrients to the un-

¹This text was submitted by the authors in English.

Abbreviations: BSCs – biological soil crusts; Car – carotenoid; Chl – chlorophyll; ETR – the relative electron transport rate; F_v/F_m – maximum quantum yield of PSII photochemistry; NPQ – non photochemical quenching; qP – photochemical quenching; Yield – actual quantum yield of PSII photochemistry.

Corresponding author: Rong Hui. Shapotou Desert Research and Experiment Station, Cold and Arid Region Environmental and Engineering Research Institute, Chinese Academy of Sciences; Donggang West Road 320, Lanzhou, Gansu, 730000 China; fax: +86 0931 4967199; e-mail: huirong850623@163.com

derlying soils, influence water runoff and vascular plant colonization, and provide favorable microhabitats for other microorganisms and protozoa [7]. Moss crusts are dominated by non-vascular plants, including *Bryum argenteum*, *Didymodon vinealis* (Brid.) Zand and *Syntrichia caninervis* Mitt. They have critical ecological functions in desert regions, and form a green bio-carpet covering large areas of land in the Tengger Desert. They are also one of the bioindicators of desertification, and are used to assess ecosystem stability and restoration success in degraded ecosystems [8]. *B. argenteum* is one of the most common species in the Tengger Desert, and usually grows in flat areas. Although moss physiological, morphological and biochemical responses to UV-B radiation or water-deficit have been extensively studied in Hungary, Australia and the United States [9], knowledge about their combined effects is extremely limited.

We hypothesized that the deleterious effects of increased UV-B may be mitigated by a concurrent water-deficit environment. Therefore, the objective of our study was to explore the interactive effects of UV-B and water-deficit on *B. argenteum* chlorophyll (Chl) fluorescence parameters; Chl, carotenoid (Car), malondialdehyde (MDA), and total flavonoid contents under a controlled environment. This study improves our understanding of the single and combined effects of increased UV-B and water-deficit under future climate change in the arid and semi-arid regions of China.

MATERIALS AND METHODS

Plant materials and experimental design. The *Bryum argenteum* crusts were selected for our study. The samples were taken from the desert steppe region at the southeastern fringe of the Tengger Desert, China (37°32'–37°36' N, 105°02'–104°30' E) in September 2011. The mean annual precipitation is 186 mm, of which 80% occurs between May and September, and the average annual temperature is 10.6°C, with a daily minimum and maximum of –25.1°C and 38.1°C, respectively. The annual evapotranspiration is approximately 3000 mm/year.

The *B. argenteum* crusts were divided into eight groups, each one consisting of six plants. In each group of samples, one of the following treatments was performed over a 10 day period: (i) well-watered with 2.75 W/m² UV-B (T_0 , control, UV-B radiation level on a clear summer day at Shapotou); (ii) well-watered with 3.08 W/m² UV-B (T_1 , equivalent to that simulated by a 6% stratospheric ozone decrease at Shapotou); (iii) well-watered with 3.25 W/m² UV-B (T_2 , equivalent to that simulated by a 9% stratospheric ozone decrease at Shapotou); (iv) well-watered with 3.41 W/m² UV-B (T_3 , equivalent to that simulated by a 12% stratospheric ozone decrease at Shapotou); (v) water-deficit with 2.75 W/m² UV-B (W, field capacity was maintained at 30% by watering); (vi) water-deficit

with 3.08 W/m² UV-B (T_1 W); (vii) water-deficit with 3.25 W/m² UV-B (T_2 W) and (viii) water-deficit with 3.41 W/m² UV-B (T_3 W).

UV-B treatments. The *B. argenteum* crusts were exposed to UV-B radiation over an 8 h (9:00–17:00) period. UV-B radiation was provided by UV-B fluorescence lamps (“Chenchen Lighting and Electronics Company”, China) that were oriented perpendicular to the sample rows and suspended above the samples. The distance between the lamps and the top of the samples was adjusted to obtain the different UV-B radiation levels. The UV-B lamps were filtered, using 0.13 mm thick cellulose acetate (“Courtaulds Chemicals”, UK), to eliminate UV-C radiation [10]. The spectral irradiance from the lamps at the sample level was determined by a UV digital spectroradiometer (“Photoelectric Instrument Factory, Beijing Normal University”, China). During the UV-B treatment, white light was also applied in order to supply photosynthetically active radiation (400–700 nm) at 150 $\mu\text{mol}/(\text{m}^2 \text{ s})$, as measured by a quantum sensor (“LI-COR”, USA).

Chl fluorescence. Chl fluorescence was measured *in situ* using a fluorimeter (PAM-2000, MFMS-2, “Hansatech”, UK) at midday. Three samples from each treatment were induced by a photon flux density equal to 400 $\mu\text{mol}/(\text{m}^2 \text{ s})$ for 5 s and then adapted to the dark for 20 min. The initial fluorescence (F_0) was determined by modulated light (<0.1 $\mu\text{mol}/(\text{m}^2 \text{ s})$) and the maximum fluorescence (F_m) was measured with a 0.8 s saturating pulse at 8000 $\mu\text{mol}/(\text{m}^2 \text{ s})$ [11, 12]. The maximum quantum yield of PSII photochemistry (F_v/F_m), the actual quantum yield of PSII photochemistry (Yield), the relative electron transport rate (ETR), photochemical quenching (qP) and non photochemical quenching (NPQ) were recorded, and calculated using the following formulas:

$$F_v/F_m = (F_m - F_0)/F_m,$$

$$\text{Yield} = (F'_m - F_t)/F'_m,$$

$$\text{ETR} = \text{Yield} \times 0.84 \times 0.5 \times \text{PPFD},$$

$$\text{qP} = (F'_m - F_s)/(F'_m - F_0),$$

$$\text{NPQ} = (F_m - F'_m)/F'_m,$$

where F_m – denotes maximal fluorescence under dark adaption, F'_m – denotes maximal fluorescence level after application of a saturating light pulse and F_t – represents the fluorescence during the steady state of photosynthesis.

Chl and Car analysis. Chl and Car were extracted from fresh material, incubated in 25 mL 100% ice cold ethanol and then centrifuged twice for 30 min at 12000 g [13]. The absorbance of the extracts was measured at 470, 649, and 665 nm with a 752 N ultraviolet

visible spectrophotometer (“Shanghai Precision and Scientific Instrument Company, Ltd”, China). Chl *a*, Chl *b*, Chl *a/b* and Car contents were calculated using the following formulas:

$$\text{Chl } a = 13.95A_{665} - 6.88A_{649},$$

$$\text{Chl } b = 24.96A_{649} - 7.32A_{665},$$

$$\text{Chl } a/b = \text{Chl } a/\text{Chl } b,$$

$$\text{Car} = (1000A_{470} - 2.05\text{Chl } a - 114\text{Chl } b)/245,$$

$$x = CVn/m,$$

where *x* – is the pigments content (mg/g fr wt), *C* – is the pigments concentration (mg/L), *V* – is the extract volume (L), *n* – is the dilution multiple, and *m* – is the fresh weight (g).

MDA analysis. MDA content was determined spectrophotometrically according to Farzadfar et al. [14]. *B. argenteum* was homogenized in 10 mL of a solution containing 10% (w/v) tri-chloroacetic acid and 0.25% (w/v) thiobarbituric acid. The mixture was heated in boiling water for 30 min and immediately cooled. The absorbance of the supernatant at 532 and 600 nm was recorded after centrifugation at 5000 g for 10 min. MDA content was calculated from the absorbance values using the following formula:

$$\text{MDA} = 6.45(A_{532} - A_{600}) V/1000 m,$$

where *V* is the extract volume (L) and *m* is the fresh weight (g).

Determination of total flavonoid content. The total flavonoid content was measured by spectrophotometry using the aluminium chloride colorimetric method [15]. Samples were extracted with 10 mL of 70% (v/w) ethanol by shaking the solutions in a water bath at 50°C for 20 min. The obtained extract was centrifuged for 10 min at 10000 g and then 1 mL of supernatant was added to a 10 mL test tube containing 1 mL of 70% (v/v) ethanol. Following this, 0.3 mL of 5% (w/v) NaNO₂ was added to the mixture and after 6 min, 0.3 mL of 10% (w/v) AlCl₃ was added. The mixture was allowed to stand for 6 min and then 2 mL of 4% (w/v) NaOH was added. After mixing, the solution was incubated for 10 min, after which, the absorbance of the reaction mixtures was measured at 510 nm and compared to a calibration curve prepared using samples containing 0, 1, 2, 3, 4, 5, 7, 10, and 15 µg of rutin. The results are expressed as milligrams of rutin equivalents per gram of fresh tissue. The total flavonoid content was calculated using the following formula:

$$\text{Total flavonoid content} = (y \times V_1 \times V_2/V_3)/m,$$

where *y* – is the flavonoids content in the samples (µg/g fr wt), *V*₁ – is the concentration of flavonoids from calibration curve (µg/mL), *V*₂ – is the volume of sample solution (mL), *V*₃ – is the constant volume of the sample (mL) and *m* is the fresh weight of sample add to the color reaction (g).

Statistical analysis. The experiment contained three replications. The Chl fluorescence, Chl, Car, MDA, and total flavonoid content values are the mean ± standard deviation (SD) of three samples. Where appropriate, the data were tested by one-way analysis of variance (ANOVA) using the SPSS 16.0 statistical package (“SPSS”, USA), followed by Duncan’s test. Differences where *P* < 0.05 were considered to be statistically significant.

RESULTS

Effects of UV-B, water-deficit and their combination on Chl fluorescence parameters

Compared to T₀, the T₁, T₂, T₃, and W treatments had significant effects on *F_v/F_m*, Yield, ETR, and qP, i.e. *F_v/F_m* decreased by 31.12, 52.36, 58.70 and 36.14%, respectively (fig. 1a). However, the UV-B and water-deficit combination treatments increased the Chl fluorescence parameters (fig. 1), and the T₁W treatment values were close to T₀. *F_v/F_m* increased more under the UV-B treatments when the crusts were well-watered, i.e. they significantly increased by 45.61, 6.502, and 22.50% for the T₁W, T₂W, and T₃W treatments when compared to T₁, T₂, and T₃, respectively (*P* < 0.05; fig. 1a). The NPQ values significantly increased under UV-B radiation or drought stress, and were 14.86% (T₁), 43.96% (T₂), 48.61% (T₃), and 26.63% (W) higher than the control (T₀) (*P* < 0.05; fig. 1e). When *B. argenteum* was exposed to the UV-B and water-deficit combination treatments, NPQ decreased by 20.49% (T₁W), 8.60% (T₂W), and 11.88% (T₃W) compared to T₁, T₂, and T₃, respectively.

Effects of UV-B, water-deficit and their combination on Chl and Car contents

UV-B alone and water-deficit alone significantly inhibited Chl *a*, Chl *b*, Chl *a/b* and Car contents. The average *B. argenteum* Chl *a* content significantly decreased by 26.15, 68.97, 74.87, and 32.56% (*P* < 0.05; fig. 2a), and Car content significantly declined by 43.87, 61.40, 67.05, and 27.81% under the T₁, T₂, T₃, and W treatments (*P* < 0.05; fig. 2d) compared to T₀, respectively. There were no significant T₁W treatment induced differences for Chl *a*, Chl *b*, Chl *a/b*, and Car content compared to the T₀. However, photosynthetic pigment contents were significantly stimulated by the UV-B and water-deficit combination. Chl *a* content increased by 37.50% for the T₁W treatment compared to T₁, 38.02% for the T₂W treatment compared to T₂, and 30.61% for the T₃W treatment (fig. 2a) compared to T₃. The Car content showed similar trends to Chl *a*, and increased by 85.47% after the T₁W treatment, 18.30% after the T₂W treatment, and 22.22% after the T₃W treatment (fig. 2d).

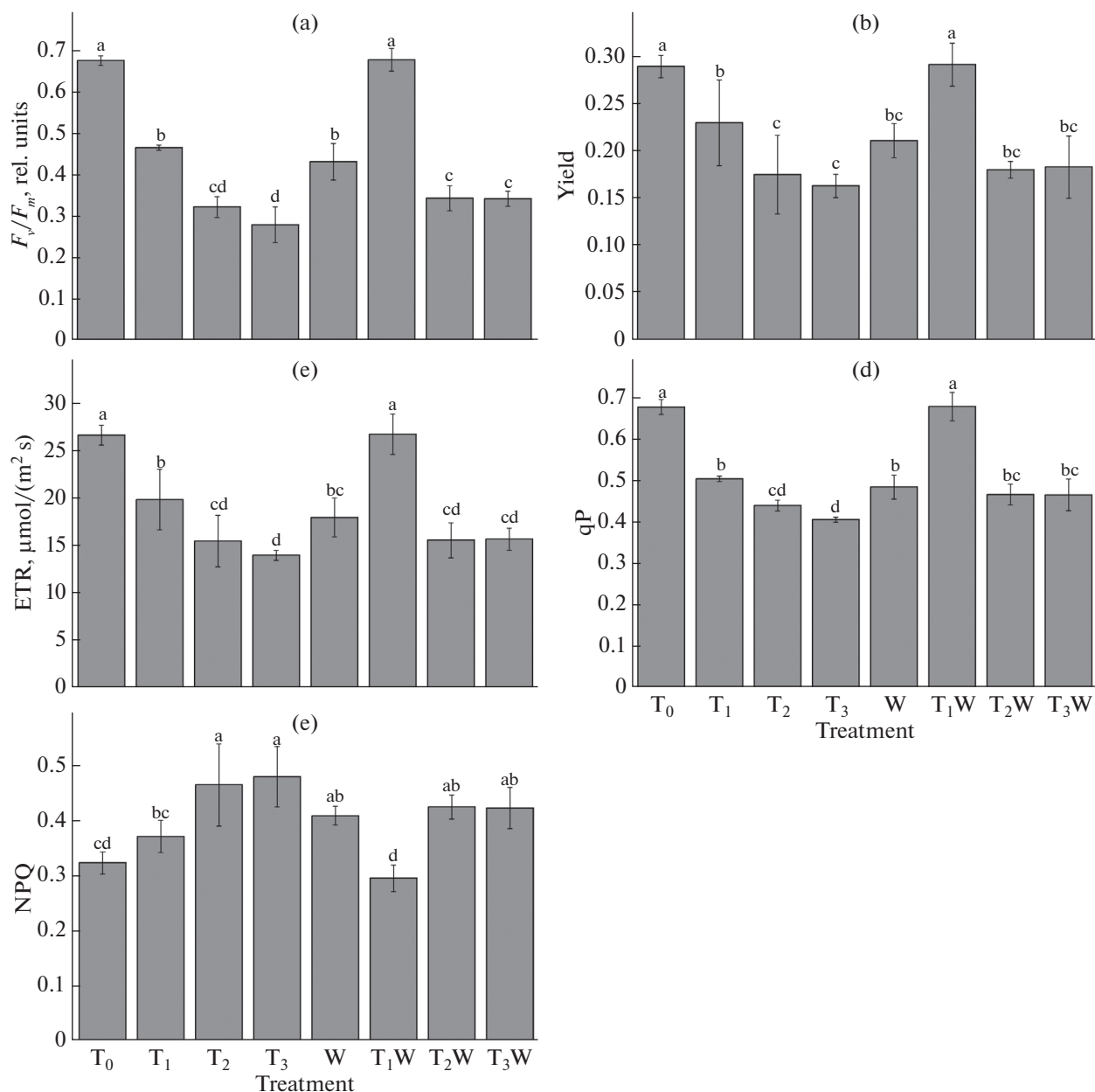


Fig. 1. F_v/F_m (a), Yield (b), ETR (c), and qP (d) values for *B. argenteum* in response to stress caused by UV-B, water-deficit, and their combination. Results represent means and standard deviation (SD) ($n \geq 3$), and different letters indicate differences at $P < 0.05$ (Duncan's test). T₀ – well-watered with 2.75 W/m² UV-B; T₁ – well-watered with 3.08 W/m² UV-B; T₂ – well-watered with 3.25 W/m² UV-B; T₃ – well-watered with 3.41 W/m² UV-B; W – water-deficit with 2.75 W/m² UV-B; T₁W – water-deficit with 3.08 W/m² UV-B; T₂W – water-deficit with 3.25 W/m² UV-B and T₃W – water-deficit with 3.41 W/m² UV-B.

Effects of UV-B, water-deficit and their combination on MDA content

UV-B or water-deficit alone increased the MDA content in *B. argenteum*. Under the T₁, T₂, T₃, and W treatments, MDA content significantly rose by 17.50, 157.5, 205.0, and 52.50% ($P < 0.05$; fig. 3) when compared to T₀, respectively. Surprisingly, MDA content after the T₁W treatment was significantly lower than

after the T₁ treatment, but was not significantly different to the T₀. Moreover, the decrease in MDA content exhibited by *B. argenteum* crusts exposed to the UV-B and water-deficit combination was similar to the well-watered crusts exposed to UV-B radiation. There were reductions of 14.89, 34.95, and 43.44% under the T₁W, T₂W, and T₃W treatments when compared to the T₁, T₂, and T₃ treatments (fig. 3), respectively.

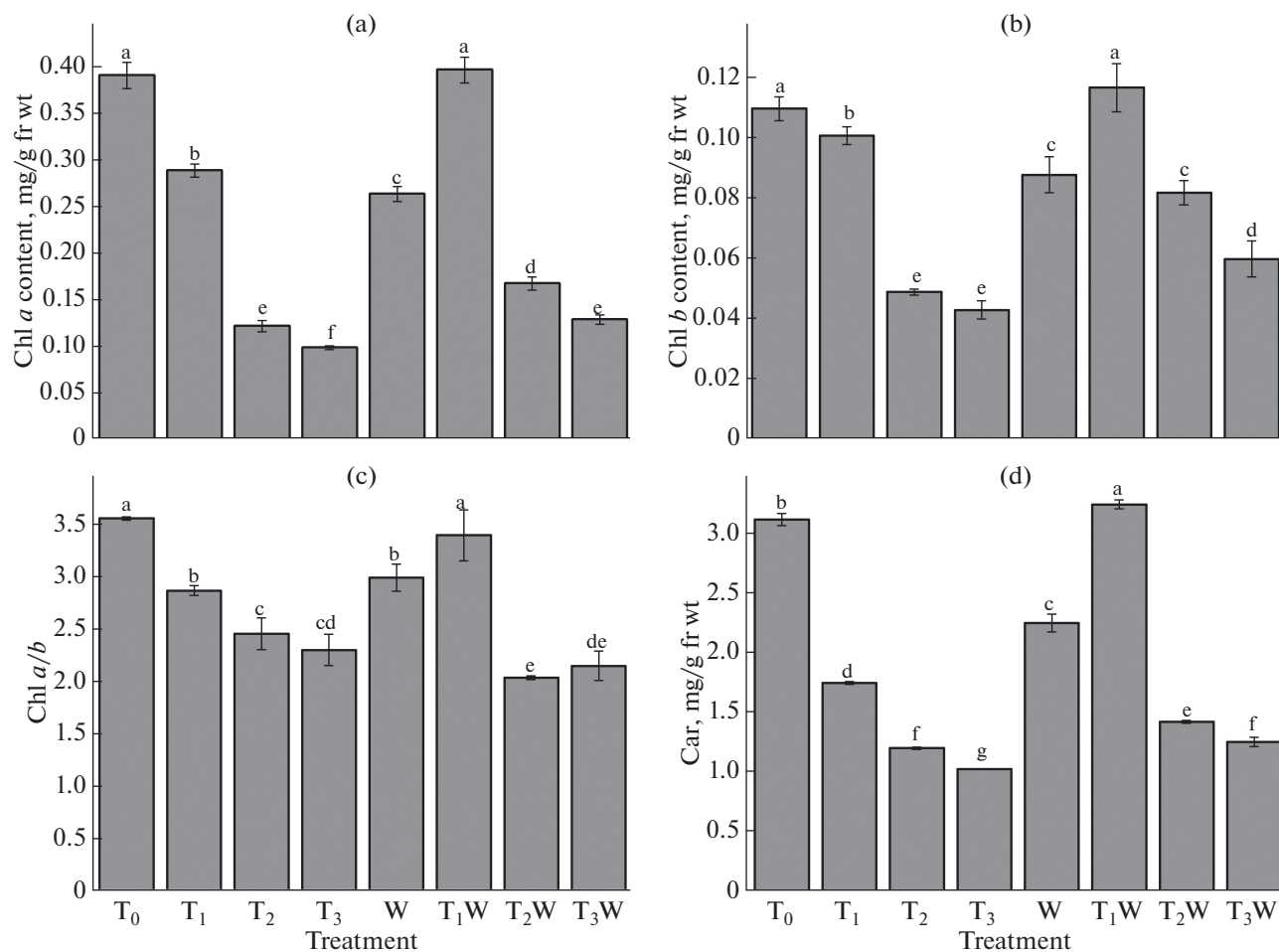


Fig. 2. Chl *a* (a), Chl *b* (b), Chl *a/b* (c), and Car (d) results for *B. argenteum* in response to UV-B and water-deficit stresses, and their combination. Designations as in fig. 1.

Effects of UV-B, water-deficit and their combination on total flavonoid content

The total flavonoid content was significantly lower in *B. argenteum* when it was exposed to UV-B or water-deficit alone, compared to the T₀. Total flavonoid content decreased by 25.08, 51.24, 67.09, and 35.78% under the T₁, T₂, T₃, and W treatments ($P < 0.05$; fig. 4), respectively. However, water-deficit treated *B. argenteum* produced significantly higher total flavonoid contents compared to the well-watered *B. argenteum* under UV-B radiation, and reached their highest values under the T₁W treatment. The increases were 44.77% for T₁W compared to T₁, 34.01% for T₂W compared to T₂, and 81.78% for T₃W compared to T₃ ($P < 0.05$; fig. 4).

DISCUSSION

The Chl fluorescence parameters are used to investigate and monitor the effect of environmental stress on photosynthesis. The F_v/F_m and Yield reflect the

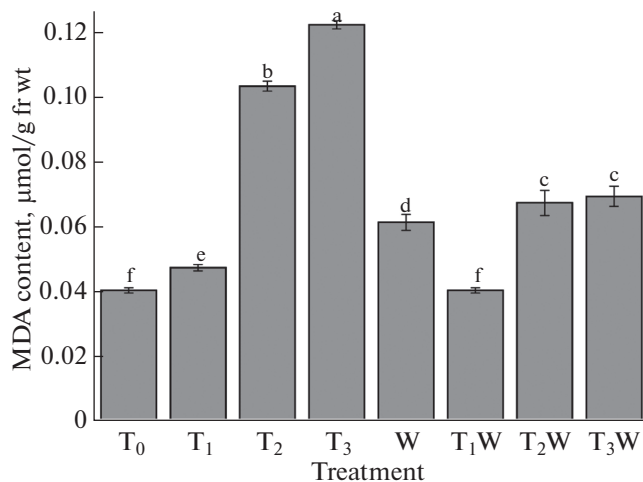


Fig. 3. *B. argenteum* MDA content when subjected to UV-B and water-deficit stresses, and their combination. Designations as in fig. 1.

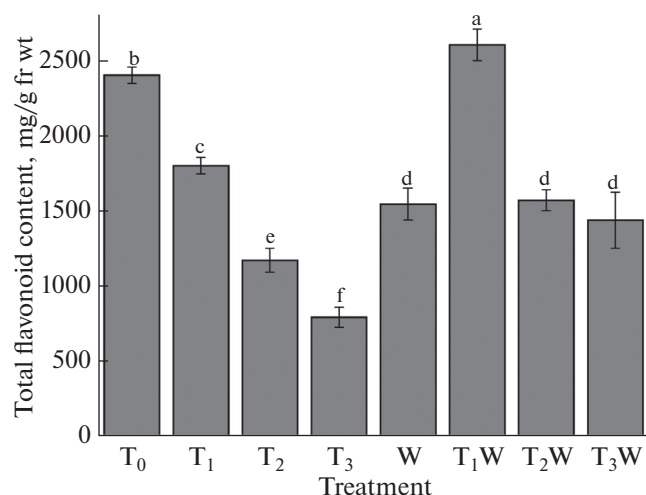


Fig. 4. *B. argenteum* total flavonoid content when subjected to UV-B and water-deficit stresses, and their combination. Designations as in fig. 1.

conversion efficiency of primary light energy and the PSII capture efficiency of primary light energy [16]. The significant reduction in F_v/F_m (fig. 1a) and Yield (fig. 1b) with increasing UV-B and water-deficit indicated that PSII was impaired in *B. argenteum* when under UV-B and water stress. The ETR is the electron transport rate of the PSII reaction center, and it represents the number and rate of light quanta that are absorbed in the electron transport process [17]. ETR was also adversely affected by UV-B and water-deficit in our experiment (fig. 1c). This response may be associated with blocking of electron transport to secondary plastiquinone [18]. The qP is regarded as an ‘indicator’ of the openness of the PSII reaction centers, while NPQ is a mechanism employed by plants to protect themselves from the adverse effects of high light intensity [19]. Our results showed that UV-B and water-deficit treatment resulted in a reduction in qP (fig. 1d) and an increase in NPQ (fig. 1e), suggesting that the PSII reaction centers had become less open, which then led to blockage in photosynthetic electron transport [20]. As the stress levels increased, the rise in NPQ can be insufficient to maintain the required number of partially oxidized PSII electron acceptors [21].

For most plants, a decrease in Chl content is one of the most common symptoms of photosynthetic damage caused by environmental stress. In our study, reductions in Chl *a*, Chl *b*, and Chl *a/b* occurred under all treatments, except for the T₁W treatment. This indicated that UV-B radiation or water-deficit alone caused more severe damage to *B. argenteum*. Our findings are in agreement with the results reported for several other species, which also indicated a significant decrease in Chl content as UV-B intensity increased [22]. A decrease in photosynthesis is often associated with a reduction in Chl pigment contents, probably caused by

suppression of Chl synthesis, accelerated Chl destruction, and/or damage to chloroplasts [23]. Moreover, our results showed that photosynthetic pigment contents were significantly stimulated by the UV-B and water-deficit combination. The masking of UV-B radiation effects in the presence of water-deficit may be due to pigment accumulation adjustments by drought, which also protect plants from UV-B radiation through various screening mechanisms [24, 25]. It is well known that pigment accumulation is an important mechanism that increases tolerance to UV-B radiation.

UV-B irradiation stress leads to disturbance of plant metabolism, which causes an increase in MDA production. The MDA level is determined by the membrane lipid peroxidation rate and is used as an indicator of membrane impairment and free radical production under stress conditions [26]. Our data showed that UV-B caused membrane damage since MDA was considerably enhanced in UV-B treated plants. The increased quantity of MDA is associated with the negative effects of UV-B on biomembrane integrity, which result in peroxidation and fragmentation of unsaturated fatty acids [27]. Furthermore, Li et al. [28] showed that drought also significantly increased MDA content. However, other results showed that combined water-deficit and UV-B treatment led to a decline in MDA content, suggesting that UV-B induced damage was partly alleviated. Similar results have been previously reported by Wang et al. [10] for maize pollen.

Carotenoids, which have a vital role in the plant response to UV-B radiation and water-deficit stresses, are a large group of isoprenoid molecules that are synthesized by all photosynthetic and non-photosynthetic organs [29]. In our study, the *B. argenteum* Car content decreased under UV-B and water-deficit, and in combination (fig. 2d). The decrease in Car content may have been caused by Car synthesis inhibition or by breakdown of Car or its precursors, which indicated that the accumulation of radical oxygen species was causing considerable oxidative stress [30]. In addition, flavonoid compounds are good radical scavengers and prevent photochemical damage [31]. Their synthesis is thought to be accelerated by UV-B radiation. Many studies have shown that there is a positive relationship between UV-B levels and flavonoid content [32]. However, our results showed that the total flavonoid content in *B. argenteum* significantly decreased as UV-B radiation, the water-deficit and their combination rose, except for the T₁W treatment (fig. 4) where the total flavonoid levels may have reached saturation point, which would stop flavonoid synthesis. In addition, the total flavonoid contents were significantly higher after the UV-B and water-deficit combination treatments than after UV-B radiation alone (fig. 4). The “first line of defense” against UV-B radiation damage induced in plants is UV-B absorbing compounds. Increased levels of UV-B absorbing compounds provide a shield against UV-B before its effects reach a sensitive target [33]. The accumulation of UV-B

absorbing flavonoids, which are effective radical scavengers, can strengthen photoprotection and reduce the effects of enhanced UV-B radiation [34].

Our results also showed that for *B. argenteum*, water-deficit was especially important in enhanced UV-B radiation environments because it can alleviate the negative effects of UV-B radiation. The reason why water-deficit can diminish the effect of UV-B radiation and why the effects depended on the dose of UV-B can be attributed to two aspects. Firstly, water-deficit considerably improves *B. argenteum*'s physiological capability to resist UV-B radiation. Water availability is the predominant limiting factor that governs desert structure and functioning. BSCs have essential ecological functions in deserts, and the fact that they can continue to grow under high UV-B levels, and at low available water levels is especially important because they can sustain their essential ecological functions when UV-B radiation is high. Alternatively, the combined action of UV-B radiation and water deficit can change the response patterns when *B. argenteum* are exposed to UV-B radiation. They can interact in additive or shielding manner during increasing stress [335]. Both the UV-B radiation and the water deficit treatments enhanced the generation of reactive oxygen species (ROS), which cause damage to proteins, lipids, carbohydrates, and DNA. Secondary metabolites accumulate in epidermal cells, which effectively screen UV-B irradiation and reduce injury to plant tissue [35]. Polyamines, tocopherol, Car, alkaloids, and flavonoids participate in the removal of ROS under increased UV-B radiation. The combination of UV-B radiation and water deficit induces responses that can be antagonistic in comparison with the action of single stresses. So water deficit may enhance resistance to UV-B radiation and *vice versa* [24].

In conclusion, UV-B radiation significantly affected Chl fluorescence parameters, photosynthetic pigment levels, and MDA and total flavonoid contents in *B. argenteum*. However, water-deficit conditions can, to some extent, help *B. argenteum* alleviate the negative effects caused by UV-B radiation. These findings further our understanding of how BSC photosynthetic capacity responds to environmental change, and provides a theoretical foundation for their assessment and protection in arid and semi-arid regions. Our understanding of the relationships between BSCs and environmental factors has substantially improved over the past few decades. However, environmental change and its impact on BSCs need to be investigated further because global climate change will become more critical in the future.

The authors gratefully acknowledge the financial support from the National Basic Research Program of China (grant no. 2013CB429906), from the National Natural Science Foundation of China (grant nos. 41271061, 41371100), and from the West Light Program for Talent Cultivation of Chinese Academy of Sciences.

REFERENCES

1. Laube J.C., Newland M.J., Hogan C., Brenninkmeijer C.A.M., Fraser P.J., Martinerie P., Oram D.E., Reeves C.E., Röckmann T., Schwander J., et al. Newly detected ozone-depleting substances in the atmosphere // Nat. Geosci. 2014. V. 7. P. 266–269.
2. Jansen M.A.K., Lemartret B., Koornneef M. Variations in constitutive and inducible UV-B tolerance; dissecting photosystem II protection in *Arabidopsis thaliana* accessions // Physiol. Plant. 2010. V. 138. P. 22–34.
3. Tegelberg R., Julkunen-Tiitto R., Vartiainen M., Paunonen R., Rousi M., Kellomäki S. Exposures to elevated CO₂, elevated temperature and enhanced UV-B radiation modify activities of polyphenol oxidase and guaiacol peroxidase and concentrations of chlorophylls, polyamines and soluble proteins in the leaves of *Betula pendula* seedlings // Environ. Exp. Bot. 2008. V. 62. P. 308–315.
4. Alexieva V., Ivanov S., Sergiev I., Karanov E. Interaction between stresses // Bulg. J. Plant Physiol. 2003. V. 29. P. 1–17.
5. Li X.R., Jia R.L., Chen Y.W., Huang L., Zhang P. Association of ant nests with successional stages of biological soil crusts in the Tengger Desert, Northern China // Appl. Soil Ecol. 2011. V. 47. P. 59–66.
6. Bowker M.A., Mau R.L., Maestre F.T., Escobar C., Castillo-Monroy A.P. Functional profiles reveal unique ecological roles of various biological soil crust organisms // Funct. Ecol. 2011. V. 25. P. 787–795.
7. Belnap J. The potential roles of biological soil crusts in dryland hydrologic cycles // Hydrol. Process. 2006. V. 20. P. 3159–3178.
8. Jia R.L., Li X.R., Liu L.C., Gao Y.H., Li X.J. Responses of biological soil crusts to sand burial in a revegetated area of the Tengger Desert, Northern China // Soil Biol. Biochem. 2008. V. 40. P. 2827–2834.
9. Karsten U., Holzinger A. Light, temperature, and desiccation effects on photosynthetic activity and drought-induced ultrastructural changes in the green alga *Klebsormidium dissectum* (Streptophyta) from a high alpine soil crust // Microb. Ecol. 2012. V. 63. P. 51–63.
10. Wang S.W., Xie B.T., Yin L.N., Duan L.S., Li Z.H., Eneji A.E., Tsuji W., Tsunekawa A. Increased UV-B radiation affects the viability, reactive oxygen species accumulation and antioxidant enzyme activities in maize (*Zea mays* L.) pollen // Photochem. Photobiol. 2010. V. 86. P. 110–116.
11. Liao J.X., Wang G.X. Effects of drought stress on leaf gas exchange and chlorophyll fluorescence of *Glycyrrhiza uralensis* // Экология. 2014. Т. 45. С. 532–538.
12. Воронин П.Ю. Установка для измерений флуоресценции хлорофилла, CO₂-газообмена и транспирации отделенного листа // Физиология растений. 2014. Т. 61. С. 291–296.
13. Lan S.B., Wu L., Zhang D.L., Hu C.X., Liu Y.D. Ethanol outperforms multiple solvents in the extraction of chlorophyll-*a* from biological soil crusts // Soil Biol. Biochem. 2011. V. 43. P. 857–861.
14. Farzadfar S., Zarinkamar F., Modarres-Sanavy S.A.M. Exogenously applied calcium alleviates cadmium toxic-

- ity in *Matricaria chamomilla* L. plants // Environ. Sci. Pollut. Res. 2013. V. 20. P. 1413–1422.
15. *Atanassova M., Georgieva S., Ivancheva K.* Total phenolic and total flavonoid contents, antioxidant capacity and biological contaminants in medicinal herbs // J. Univ. Chem. Technol. Metallurgy. 2011. V. 46. P. 81–88.
 16. *Guidi L., Mori S., Degl'Innocenti E., Pecchia S.* Effects of ozone exposure or fungal pathogen on white lupin leaves as determined by imaging of chlorophyll *a* fluorescence // Plant Physiol. Biochem. 2007. V. 45. P. 851–857.
 17. *Kitajima M., Butler W.L.* Excitation spectra for photosystem I and photosystem II in chloroplasts and the spectral characteristics of the distributions of quanta between the two photosystems // Biochim. Biophys. Acta. 1975. V. 408. P. 297–305.
 18. *Huang J.L., Silva E.N., Shen Z.G., Jiang B., Lu H.F.* Effects of glyphosate on photosynthesis, chlorophyll fluorescence and physicochemical properties of cogon-grass (*Imperata cylindrical* L.) // Plant Omics J. 2012. V. 5. P. 177–183.
 19. *Samoilova O.P., Ptushenko W., Kuvykin I.V., Kiselev S.A., Ptushenko O.S., Tikhonov A.N.* Effects of light environment on the induction of chlorophyll fluorescence in leaves: a comparative study of *Tradescantia* species of different ecotypes // Biosystems. 2011. V. 105. P. 41–48.
 20. *Li G.L., Wu H.X., Sun Y.Q., Zhang S.Y.* Response of chlorophyll fluorescence parameters to drought stress in sugar beet seedlings // Физиология растений. 2013. T. 60. C. 345–350.
 21. *Li Q.M., Liu B.B., Wu Y., Zou Z.R.* Interactive effects of drought stresses and elevated CO₂ concentration on photochemistry efficiency of cucumber seedlings // J. Integr. Plant Biol. 2008. V. 50. P. 1307–1317.
 22. *Liu Q., Yao X.Q., Zhao C.Z., Cheng X.Y.* Effects of enhanced UV-B radiation on growth and photosynthetic responses of four species of seedlings in subalpine forests of the eastern Tibet plateau // Environ. Exp. Bot. 2011. V. 74. P. 151–156.
 23. *Javadmanesh S., Rahmani F., Pourakbar L.* UV-B radiation, soil salinity, drought stress and their concurrent effects on some physiological parameters in maize plant // American-Eurasian J. Toxicol. Sci. 2012. V. 4. P. 154–164.
 24. *Basahi J.M., Ismail I.M., Hassan I.A.* Effects of enhanced UV-B radiation and drought stress on photosynthetic performance of lettuce (*Lactuca sativa* L. Romaine) plants // Annu. Rev. Res. Biol. 2014. V. 4. P. 1739–1756.
 25. *Pandey N., Pandey-Rai S.* Modulations of physiological responses and possible involvement of defense-related secondary metabolites in acclimation of *Artemisia annua* L. against short-term UV-B radiation // Planta. 2014. V. 240. P. 611–627.
 26. *Katsuhara M., Otsuka T., Ezaki B.* Salt stress-induced lipid peroxidation is reduced by glutathione S-transferase, but this reduction of lipid peroxides is not enough for recovery of root growth in *Arabidopsis* // Plant Sci. 2005. V. 169. P. 369–373.
 27. *Kramer G., Norman H., Krizek D., Mirecki R.* Influence of UV-B radiation on polyamines, lipid peroxidation and membrane lipids in cucumber // Phytochemistry. 1991. V. 30. P. 2101–2108.
 28. *Li Y., Zhao H.X., Duan B.L., Korpelainen H., Li C.Y.* Effect of drought and ABA on growth, photosynthesis and antioxidant system of *Cotinus coggygria* seedlings under two different light conditions // Environ. Exp. Bot. 2011. V. 71. P. 107–113.
 29. *Simkin A.J., Moreau H., Kuntz M., Pagny G., Lin C., Tanksley S., McCarthy J.* An investigation of carotenoid biosynthesis in *Coffea canephora* and *Coffea arabica* // J. Plant Physiol. 2008. V. 165. P. 1087–1106.
 30. *Singh R., Singh S., Tripathi R., Agrawal S.B.* Supplemental UV-B radiation induced changes in growth, pigments and antioxidant pool of bean (*Dolichos lablab*) under field conditions // J. Environ. Biol. 2011. V. 32. P. 139–145.
 31. *Ryan K., Burne A., Seppelt R.D.* Historical ozone concentrations and flavonoid levels in herbarium specimens of the antarctic moss *Bryum argenteum* // Global Change Biol. 2009. V. 15. P. 1694–1702.
 32. *Eichholz I., Rohn S., Gamm A., Beesk N., Herppich W.B., Kroh L.W., Ulrichs C., Huyskens-Keil S.* UV-B-mediated flavonoid synthesis in white asparagus (*Asparagus officinalis* L.) // Food Res. Int. 2012. V. 48. P. 196–201.
 33. *Shen X., Dong Z., Chen Y.* Drought and UV-B radiation effect on photosynthesis and antioxidant parameters in soybean and maize // Acta Physiol. Plant. 2015. V. 37. P. 1–8.
 34. *Kumari R., Agrawal S.B.* Supplemental UV-B induced changes in leaf morphology, physiology and secondary metabolites of an Indian aromatic plant *Cymbopogon citratus* (D.C.) Stapf under natural field conditions // Int. J. Environ. Stud. 2010. V. 67. P. 655–675.
 35. *Bandurska H., Niedziela J., Chadzinikolau T.* Separate and combined responses to water deficit and UV-B radiation // Plant Sci. 2013. V. 213. P. 98–105.